

Skin Currents and Compound Sawteeth in Tokamaks

Richard E. Denton, J. F. Drake, Robert G. Kleva, and D. A. Boyd

Laboratory for Plasma and Fusion Energy Studies, University of Maryland, College Park, Maryland 20742
(Received 13 January 1986)

Two-dimensional MHD simulations are carried out which demonstrate that the cross-field thermal conduction near the magnetic axis controls the structure of sawteeth in tokamaks. In simulations of discharges with good central confinement, skin currents form at a finite radius causing the safety factor q to fall below 1 away from the magnetic axis. Both normal and compound sawteeth are produced which have many features consistent with experimental observations.

PACS numbers: 52.30.-q, 52.55.Fa, 52.65.+z

Sawteeth¹ are a common feature of nearly all tokamak experiments. The central temperature drops in a sudden crash and then rises slowly until the next crash. In Kadomtsev's sawtooth model² when $q(0) = q(r=0) < 1$, the $m=1$ tearing mode grows to large amplitude, driving $q(0)$ above 1 and flattening the central-temperature profile. Here, the safety factor is $q(r) = rB_z/RB_\theta$, where B_z and B_θ are the toroidal and poloidal magnetic fields and R is the major radius. After the crash Ohmic heating increases the central temperature (and conductivity). The central current density $J(0)$ then increases and $q(0) [\propto J(0)^{-1}]$ falls until $q(0) < 1$ at which time the cycle repeats. In MHD simulations in which the electron temperature T was evolved self-consistently, however, sawteeth were only seen as a transient before decaying away.³ In these computations, however, parallel thermal conduction $\kappa_{||}$ was not included. Recently we have carried out computations with $\kappa_{||}$ and have shown that the decay of the sawteeth was caused by the formation of an $m=1$ convection cell at the center of the plasma column.⁴ For sufficiently large values of $\kappa_{||}$, periodic sawteeth were produced which were in accord with the Kadomtsev model.

While the qualitative features of the sawteeth in our simulations were consistent with the experimental measurements of normal sawteeth, there were a number of significant discrepancies with the observations. Moreover, we were never able to produce the compound sawteeth which were reported in the Doublet III tokamak⁵ and the Texas experimental tokamak (TEXT)⁶ and are now observed in the larger tokamaks.^{7,8}

In the present manuscript we show that the nature of the sawteeth in our simulations can be changed by altering the form of the perpendicular thermal conduction κ_{\perp} , which was previously taken as a constant. In particular, we consider a simple model in which κ_{\perp} is small near the magnetic axis and is large at the plasma edge. The sawteeth then differ significantly from the original Kadomtsev model: q remains around or above 1 near $r=0$ but falls below 1 at a finite radius as a result of the formation of skin currents. Our simulations reproduce many features of the experimental ob-

servations including both normal and compound sawteeth.

Our calculations are based on the reduced resistive MHD equations for helical perturbations in cylindrical geometry,⁹

$$d\nabla_{\perp}^2\phi/dt - \mu\nabla_{\perp}^4\phi = \tilde{\mathbf{B}} \cdot \nabla J, \quad (1)$$

$$\nabla_{\perp}^2\psi = J - 2n/m, \quad (2)$$

$$\partial\psi/\partial t = \tilde{\mathbf{B}} \cdot \nabla\phi + \eta J, \quad (3)$$

where $d/dt = \partial/\partial t + \mathbf{v} \cdot \nabla$, J is the axial current, and the velocity \mathbf{v} and magnetic field \mathbf{B} are given by $\mathbf{v} = \hat{\mathbf{z}} \times \nabla\phi$ and $\mathbf{B} = \hat{\mathbf{z}} + (nr/m)\hat{\theta} + \hat{\mathbf{z}} \times \nabla\psi$, with ϕ and ψ the stream function and helical flux function, respectively. The equations are written in normalized units: $t/\tau_A \rightarrow t$, $a\nabla_{\perp} \rightarrow \nabla_{\perp}$, $R\partial/\partial z \rightarrow \partial/\partial z$, and $\eta\tau_A c^2/4\pi a^2 \rightarrow \eta$, where $c_A = (B_z^2/Mn)^{1/2}$ is the Alfvén velocity, $\tau_A = R/c_A$ is the Alfvén time, η is the resistivity, μ is the viscosity, a is the minor radius, $2\pi R$ is the periodicity length in z , and $n/m=1$ is the pitch of the perturbation ($m\partial/\partial z = -n\partial/\partial\theta$). The resistivity is evolved self-consistently with the temperature by use of the classical relationship $\eta = \hat{\eta}/T^{3/2}$ with

$$dT/dt - \kappa_{\perp}\nabla_{\perp}^2 T - \kappa_{||}(\tilde{\mathbf{B}} \cdot \nabla)^2 T = \Omega\eta J^2, \quad (4)$$

where κ_{\perp} and $\kappa_{||}$ are the perpendicular and parallel rates of thermal conduction, $\Omega = a^2 B_z^2/4\pi n\hat{T}R^2$ is the ratio of the resistive time to the Ohmic heating time, and $T/\hat{T} \rightarrow T$ with \hat{T} an arbitrary normalization for T . The parameters $\kappa_{||}$, Ω , and $\hat{\eta}$ are time and space independent. The perpendicular conduction is taken to be

$$\kappa_{\perp} = \kappa_{\perp 0}(1 + \alpha|\nabla T|^2), \quad (5)$$

where $\kappa_{\perp 0}$ and α are constants. Since at the present time there is no accepted theory of anomalous transport, there is no theoretical justification for the expression given in Eq. (5). However, this form results in a larger value of κ_{\perp} at the edge than in the center ($\kappa_{\perp 0}$) as is experimentally observed and allows the central region of small κ_{\perp} to adjust with the width of the temperature profile. The parameters $\kappa_{\perp 0}$ and α control the

widths of the J and T profiles which result once a steady-state sawtoothing plasma column has been established. A large value of $\kappa_{\perp 0}$ or α corresponds to a narrow profile and vice versa.

We solve Eqs. (1)–(5) by expanding in harmonics in the poloidal plane, finite differencing in the radial direction (with typically 50–150 radial grid points), and then advancing the equations with a semi-implicit scheme. The number of harmonics retained at any given time during a run is adjusted automatically to maintain accuracy. Typically only three harmonics are kept between sawtooth crashes while during a crash up to nine harmonics are retained.

In Fig. 1(a) we show $T(0)$, $T(0.20)$, and $T(0.28)$ versus time for a typical run with a constant κ_{\perp} ($\alpha=0$). Other parameters are $\Omega=1$, $\kappa_{\parallel}=60$, $\kappa_{\perp 0}=3.7 \times 10^{-6}$, and $\hat{\eta}=\mu=2.0 \times 10^{-5}$. In presenting the data in Fig. 1 we have rotated the plasma column with a period of 240 to model the corresponding rotation in the actual experiment. Thus, the traces in Fig. 1 model the time dependence of the signal from an electron-cyclotron-emission measurement of the local temperature. The three traces exhibit the qualitative features of normal sawteeth: The periodic crash of $T(0)$ is closely followed by a rise in $T(0.28)$. The oscillation in $T(0.20)$ preceding the sawtooth crash is caused by the $m/n=1$ magnetic island which grows to large amplitude and drives the hot central plasma toward the wall. In Fig. 2 we show cuts of the (a)

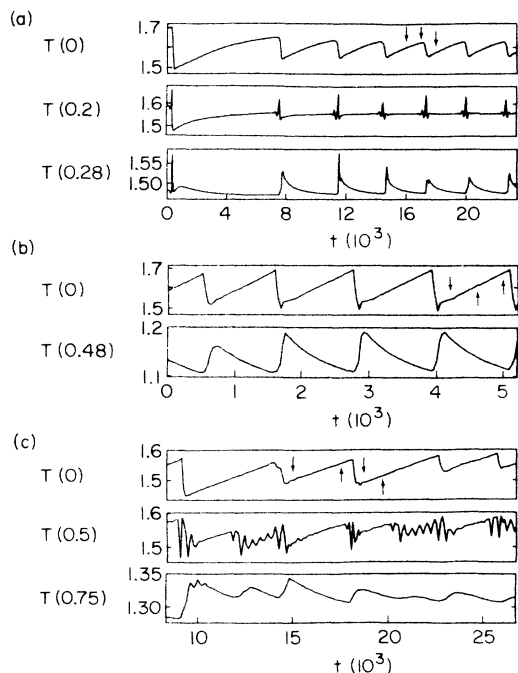


FIG. 1. Evolution of the electron temperature for (a) normal sawteeth and constant κ_{\perp} at $r=0$, 0.20, and 0.28; (b) normal sawteeth with small $\kappa_{\perp 0}$ at $r=0$ and 0.48; and (c) normal and compound sawteeth with small $\kappa_{\perp 0}$ at $r=0$, 0.50, and 0.75.

current profile and (b) temperature profile halfway up the sawtooth rise (curves 1), just prior to the crash (curves 2), and just after the crash (curves 3) [see arrows in Fig. 1(a)]. Only the interior ($r < 0.5$) of the plasma column is shown so that the detailed profiles can be more clearly seen. Before the crash J is peaked with $J(0) > 2$ so that $q(0) = 2/J(0) < 1$. After the crash J is flattened with $J(0) \leq 2$ so that $q(0) \geq 1$. The temperature is also peaked prior to the crash and is flattened afterwards.

These sawteeth are consistent with the Kadomtsev model.² However, there are a number of discrepancies with the experimental observations. First, the rate of rise of $T(0)$ in Fig. 1(a) decreases significantly during the sawtooth rise, producing distinctly rounded sawteeth. Perpendicular transport near the magnetic axis begins to conduct energy out of the center and this reduces $\partial T(0)/\partial t$. In experimental observations, on the other hand, $T(0)$ typically rises uniformly until the crash. Rounded sawteeth are seen occasionally, but are not the norm.

Second, recent electron-cyclotron-emission measurements of the electron temperature on sawtoothing discharges in the Princeton tokamak fusion test reactor (TFTR) indicate that the profiles are often distinctly hollow just after the sawtooth crash.¹⁰ In Fig. 3 we show typical experimental measurements of $T(R)$ during the rise of the sawtooth (dashed), 21 ms later just before a sawtooth crash (solid), and 12 ms later after the crash (dotted). In our simulations with constant κ_{\perp} the $m=1$ tearing mode causes the hot central plasma to mix with the colder plasma at larger radii, producing final temperature profiles which are nearly flat across the center. Hollow profiles have only been observed when the convective flow dominates parallel

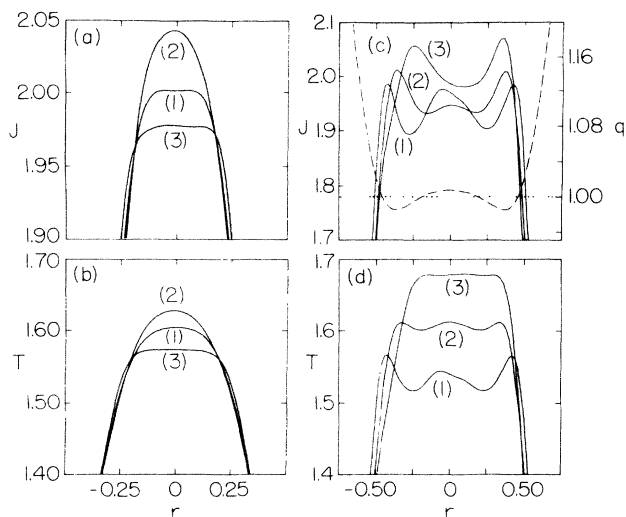


FIG. 2. Evolution of J and T profiles during normal sawteeth (a), (b) with constant κ_{\perp} and (c), (d) with small $\kappa_{\perp 0}$. The dashed curve in (c) is the q profile.

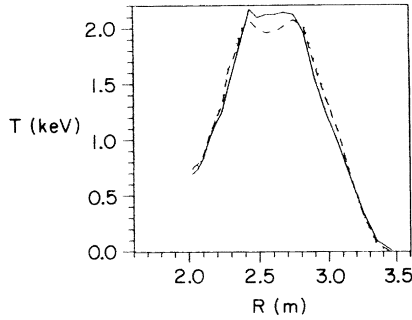


FIG. 3. Electron-cyclotron-emission measurement of the electron temperature profiles in TFTR.

conduction, i.e., κ_{\parallel} is unrealistically small.

Third, we have never been able to produce the compound sawteeth that have recently been seen experimentally, even after having varied $\hat{\eta}$, Ω , and $\kappa_{\perp 0}$ over a wide range.

We now demonstrate that by simply reducing κ_{\perp} around the center of the plasma column by decreasing $\kappa_{\perp 0}$ and increasing α we produce both normal and compound sawteeth in which these discrepancies are eliminated. In Fig. 1(b) we show $T(0)$ and $T(0.48)$ versus time for a run with $\Omega = 1$, $\kappa_{\parallel} = 40$, $\kappa_{\perp 0} = 7.5 \times 10^{-6}$, $\alpha = 0.27$, and $\hat{\eta} = \mu = 1.0 \times 10^{-4}$. Several sawteeth preceded those shown in Fig. 1(b). In all of the sawteeth the rate of rise of $T(0)$ is nearly constant until the crash, consistent with observations. In Fig. 2 we show cuts of (c) J and (d) T after the crash, during the rise of the next sawtooth, and just prior to the next crash [see arrows in Fig. 1(b)]. After the sawtooth crash, the T profile is distinctly hollow and gradually becomes flatter during the rise of the sawtooth. The hollow temperature profile after the crash causes skin currents to develop. Just after the crash in Fig. 2(c), the central current is reduced with $q \geq 1$. Note, however, that J is not flattened around $r = 0$. During the rise of the sawtooth, skin currents grow stronger and become more pronounced. The q profile just prior to the crash is also shown in Fig. 2(c). The skin currents cause q to fall below 1 away from the magnetic axis while $q(0) \geq 1$. The magnetic islands which grow on the resulting double q profile do not grow to the magnetic axis if $q(0)$ is sufficiently far above 1.¹¹ However, the results presented in Fig. 1(b) are for a rather large value of resistivity ($\eta \sim 10^{-4}$) so that the time scale for the growth of the magnetic islands^{12,13} ($\sim \eta^{-1/3}$) is comparable to the time required for $q(0)$ to fall to unity. As a consequence, the magnetic island of the tearing mode grows until it expels the entire central plasma and produces a normal sawtooth crash.

The formation of the hollow temperature profile after the sawtooth crash can be simply understood. Since $q(0) \sim 1$ in the vicinity of the magnetic axis,

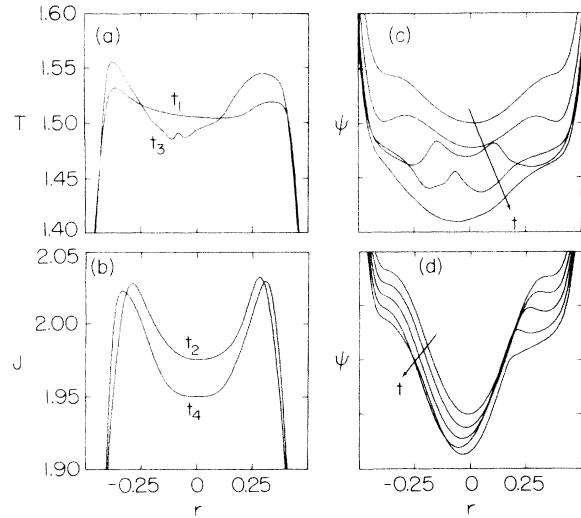


FIG. 4. Profiles of (a) T , (b) J , and (c), (d) ψ during compound sawteeth [Fig. 1(c)]. The evolution of ψ is shown during (c) the normal crash around $t = 1.8 \times 10^4$ and (d) the subordinate crash around $t = 2.0 \times 10^4$.

very little helical flux links the hot central plasma [from Eq. (2), $\nabla_{\perp}^2 \psi \approx 0$]. As the hot central plasma is expelled from the center, it cannot reconnect with the cold plasma at larger radii so that no mixing of the hot and cold plasma occurs. The central plasma simply redistributes as a hot ring as seen in Fig. 2(d).

Compound sawteeth occur at lower values of the resistivity. In Fig. 1(c) we show $T(0)$, $T(0.5)$, and $T(0.75)$ for a run with $\Omega = 1$, $\kappa_{\parallel} = 100$, $\kappa_{\perp 0} = 1.0 \times 10^{-6}$, $\alpha = 0.2$, and $\hat{\eta} = \mu = 1.0 \times 10^{-5}$. The data are rotated with a period of 400. Several sawteeth preceded those shown in Fig. 1(c). Of the four sawteeth shown, the first and third are compound and the second and fourth are normal. The period of the compound sawteeth is approximately 50% longer than that of the normal sawteeth. Bursts of MHD activity are clearly visible in the middle trace beginning about halfway up each of the compound sawteeth. A corresponding heat pulse associated with this subordinate crash appears on the outer trace. The central temperature is unaffected. The successor oscillations from the subordinate crashes have much longer lifetimes than the successor from the main crashes.

Figure 4 illustrates the nature of the alternating normal-compound sawtooth cycle which appears in Fig. 1(c). In Fig. 4 we show cuts of (a) T at $t_1 = 1.5 \times 10^4$ and $t_3 = 1.87 \times 10^4$ and (b) J at $t_2 = 1.75 \times 10^4$ and $t_4 = 1.97 \times 10^4$. At the beginning of the first normal sawtooth at t_1 , the central temperature is only slightly hollow. During the rise of this sawtooth, skin currents form as can be seen at t_2 , just prior to the crash. Cuts of the helical flux are shown in Fig. 4(c) at several times around this crash. The ra-

tional surface $q = 1$ is defined by $\partial\psi/\partial r = 0$ (excluding the origin). Two $q = 1$ surfaces form around $r = 0.37$. The double tearing mode growing on this q profile will remain localized away from $r = 0$ and therefore will not affect $T(0)$ if $\psi_{\min} > \psi(r = 0)$, where ψ_{\min} is the secondary minimum of ψ at the outermost rational surface.¹¹ In Fig. 4(c) ψ_{\min} drops until $\psi_{\min} \leq \psi(0)$ so the mode grows until it encompasses the magnetic axis and produces a normal crash. The skin currents at this time were too weak to cause a subordinate crash. Just after this crash at t_3 the temperature profile, shown in Fig. 4(a), is distinctly hollow (see previous discussion) and consequently by t_4 rather strong skin currents [Fig. 4(b)] have formed. Cuts of the helical flux function around this time are shown in Fig. 4(d). In this case $\psi_{\min} \gg \psi(r = 0)$ so that the mode is localized away from the magnetic axis, and therefore produces a subordinate relaxation. This subordinate crash is caused by a localized $m/n = 1$ resistivity-gradient-driven mode rather than the double tearing mode. At $t = 2.1 \times 10^4$, after the subordinate crash, both T and J are rather flat and by the time of the main crash at $t = 2.26 \times 10^4$ only a very small skin current has formed. The $m = 1$ mode therefore grows until it encompasses the entire central region and flattens T and J .

The formation of compound sawteeth requires a skin current as well as a sufficiently small value of resistivity so that the time scales for resistive-mode growth and background-profile evolution are well separated. In our simulations the minimum resistivity is of the order of 10^{-5} . The development of skin currents requires a flat or hollow temperature profile, which is controlled by $\kappa_{\perp 0}$, the central rate of perpendicular conduction. In particular, the parameter $\kappa_{\perp 0} \tau_h / r_I^2$, with $\tau_h = (\hat{\eta} \Omega)^{-1}$ the central Ohmic heating time and r_I the sawtooth inversion radius, appears to determine the existence of skin currents. For the run with $\hat{\eta} = 10^{-4}$ shown in Fig. 1(b) the skin currents are moderately well developed. At larger values of $\kappa_{\perp 0}$ or smaller r_I no skin currents are observed and the sawteeth eventually become rounded for sufficiently large $\kappa_{\perp 0}$. For smaller $\kappa_{\perp 0}$ or larger r_I the skin currents are more pronounced. A run with $\hat{\eta} = 10^{-5}$ similar to that shown in Fig. 1(c) but with a narrower profile ($\kappa_{\perp 0} = 1.08 \times 10^{-6}$) produced weaker skin currents and did not form compound sawteeth. It should be emphasized that a peaked impurity profile can also cause skin currents. In future studies we will

investigate the role of impurity dynamics, the range of parameters over which compound sawteeth appear, and the scaling of the sawtooth repetition and crash times with η so that our results can be extrapolated to the present high-temperature tokamak regime where $\eta \sim 10^{-6} - 10^{-8}$.

We have shown that the cross-field thermal conduction near the magnetic axis controls the structure of sawteeth in tokamak discharges. In our simulations normal sawteeth occur when moderate skin currents form which drive q below 1 at a finite radius away from the magnetic axis. The resulting sawtooth crashes can produce hollow temperature profiles. In simulations with low edge q (broad current profiles) and very good central confinement, strong skin currents develop and produce compound sawteeth.

We would like to thank K. McGuire and J. M. Finn for helpful discussions. This work was supported in part by the U. S. Department of Energy.

¹S. Von Goeler, W. Stodiek, and N. R. Sauthoff, Phys. Rev. Lett. **33**, 1201 (1974).

²B. B. Kadomtsev, Fiz. Plazmy **1**, 710 (1975) [Sov. J. Plasma Phys. **1**, 389 (1975)].

³A. Sykes and J. A. Wesson, Phys. Rev. Lett. **37**, 140 (1976).

⁴R. E. Denton, J. F. Drake, and R. G. Kleva, to be published.

⁵W. Pfeiffer, Nucl. Fusion **25**, 673 (1985).

⁶J. A. Snipes, T. P. Kochanski, and S. B. Kim, University of Texas Fusion Research Center Report No. 255, 1983 (unpublished); S. B. Kim, private communication.

⁷H. Yamada, K. McGuire, D. Colchin, P. C. Efthimion, E. Frederickson, K. Hill, J. Kiraly, V. Pare, G. Taylor, and N. Sauthoff, Princeton Plasma Physics Laboratory Report No. 2213 (unpublished).

⁸D. J. Campbell *et al.*, in Proceedings of the Twelfth European Conference on Controlled Fusion and Applied Plasma Physics, Budapest, Hungary 2-6 September 1985 (to be published).

⁹M. N. Rosenbluth, D. A. Monticello, H. R. Strauss, and R. B. White, Phys. Fluids **19**, 1987 (1976).

¹⁰D. A. Boyd, private communication.

¹¹V. V. Parail and G. V. Pereverzev, Fiz. Plazmy **6**, 27 (1980) [Sov. J. Plasma Phys. **6**, 14 (1980)].

¹²B. Coppi, R. Galvão, R. Pellat, M. N. Rosenbluth, and P. H. Rutherford, Fiz. Plazmy **2**, 961 (1976) [Sov. J. Plasma Phys. **2**, 533 (1976)].

¹³P. L. Pritchett, Y. C. Lee, and J. F. Drake, Phys. Fluids **23**, 1368 (1980).